



Adsorption of methylene blue by seed husks of *Moringa oleifera* Lam

B.R.R. Alves^a, R.A. Konzen*, R.C.P.R. Domingues, F.J. Bassetti, L.A. Coral

^aAcademic Department of Chemistry and Biology, Federal University of Technology - Paraná (UTFPR), Campo Comprido, ZIP Code: 81280-340, 5000 Curitiba-PR, Brazil, emails: raquelkonzen1@gmail.com (R.A. Konzen), reisalvesb@gmail.com (B.R.R. Alves), robertac@utfpr.edu.br (R.C.P.R. Domingues), bassetti@utfpr.edu.br (F.J. Bassetti), lucilacoral@utfpr.edu.br (L.A. Coral)

^bFederal University of Technology – Paraná (UTFPR) – Environmental Sciences and Technology Graduate Program, Deputado Heitor de Alencar Furtado St., 5000 Ecoville, Postal Code: 81280-340, Curitiba, Paraná, Brazil

Received 19 November 2019; Accepted 20 March 2020

ABSTRACT

The discharge of great volumes of wastewater containing dyes is a problem concerning many industries, and removing these compounds effectively is essential. Many parts of the plant *Moringa oleifera* Lam (MO) are being investigated as low-cost alternatives in adsorption processes. MO seed husks were employed in this study to remove methylene blue (MB) from water. Minimum preparation was employed to use MO seed husks in adsorption of MB. Equilibrium was achieved in 90 min, and kinetic data was better described by the Avrami model. The adsorption isotherm was better described by Langmuir, with a maximum adsorption capacity (q_{max}) of 69.73 mg g⁻¹ at 298 K. Thermodynamic calculations were also employed, indicating that removal of MB by MO seed husks is a spontaneous reaction. The adsorbent was successfully applied to remove MB from water. Seed husks of MO can be considered a low-cost and widely available alternative to water and wastewater treatment systems.

Keywords: Bio-sorbent; Dye removal; Moringa seed waste; Water treatment

1. Introduction

Dyes are extensively applied in various industrial segments, such as textile, food, and pharmaceutical production. In the textile industry, 1%–15% of dyes applied are lost and becomes part of the effluent during the coloring process [1,2], causing harmful effects in aquatic environments, as they can hinder photosynthesis, increase electrical conductivity, chemical, and biochemical oxygen demand, and cause teratogenic and carcinogenic effects to the living organisms [1,3,4]. The most frequently used cationic dye in the coloration of cotton, wool, and silk is methylene blue (MB) [5]. MB can cause harmful effects in humans when ingested, such as nausea, burn sensations, vomiting, increased heart rate, cyanosis, tissue necrosis, and mental confusion [6,7].

Many conventional treatment technologies such as Fenton, electrochemical processes, biodegradation, ultra-filtration,

coagulation, sedimentation, and filtration have been investigated extensively [6]. However, these processes do not produce satisfactory results to remove dyes since most of these compounds are resistant, due to their complex molecular structure, which provides stability and low biodegradability characteristics. Among conventional methods, adsorption is promising in terms of efficiency [3,8–10]. Nevertheless, limiting its use is the fact that activated carbon, the most used adsorbent, is expensive, which prompt many researchers to investigate low-cost alternative materials [3].

Moringa oleifera Lam (MO) is a plant found in many tropical and subtropical regions. Many parts of this plant are used in human and animal nutrition, including its fruits, flowers, leaves, and pods [11,12]. In water treatment, MO extracts are being successfully used as a low-cost coagulant [13], and evidence of antibacterial properties already exists [11]. MO seed powder was successfully employed to eradicate pathogenic bacterial strains in the form of a dip bag, reaching 99.9% eradication in 5 min, using 100 mg of MO seed powder [14].

* Corresponding author.

In adsorption, several studies have utilized MO for preparing activated carbons and bio-sorbents to remove a variety of pollutants, such as nitrate [15], heavy metals [16], diuron [17], and tartrazine [18]. MO seed husks, however, are normally treated as by-product, although they also possess great potential for use in adsorption [19,20]. Its use can improve water treatment in poor countries and, at the same time, provide a source of income based on a material otherwise discarded.

The present study evaluated MO seed husks as an adsorbent to remove dyes from water. Methylene blue (MB) was selected as a model dye to examine the adsorption and applicability of MO seed husks to mitigate environmental impacts from this contaminant in water.

2. Materials and methods

2.1. Materials

MB was purchased from Biotec® and used without further purification. MB main physicochemical properties can be seen in Table 1.

Seed husk of MO was used as an adsorbent to remove MB from water. Soluble impurities were removed by washing the material with deionized water, followed by drying at 110°C for 24 h. The material was grounded and sieved through five openings: 10, 60, 80, 100, and 150 Tyler mesh sizes. Activated carbon can be considered granular when at least 90% (m/m) of the carbonized sample is retained by an 80 mesh sieve (0.177 mm) [22]. In this study, particle sizes in the range of 0.1–2.0 mm (10–100 mesh) were collected. This material was employed in further experiments and classified as a granular adsorbent.

2.2. Methods

2.2.1. Characterization techniques

Fourier transform infrared spectroscopy (Varian 640-IR) was used to determine surface functional groups, and employed using attenuated total reflectance (ATR) and KBr discs. The adsorbent was dried at 110°C previous to this analysis in order to remove water. The adsorbent was mixed with dried KBr using an agate mortar and pestle, and sample discs

were prepared using a manual press. Samples were analyzed in the region of 4,000–650 cm⁻¹.

Acidic and basic oxygen surface groups were detected by Boehm titration [23,24]. To perform Boehm's method, 0.5 g of MO were added in four Erlenmeyer flasks containing 50 mL of the following solutions: 0.1 mol L⁻¹ of sodium hydroxide (NaOH), sodium carbonate (Na₂CO₃), sodium bicarbonate (NaHCO₃), and chloridric acid (HCl). These flasks were sealed and placed in an incubator shaker for 24 h. After this period, samples were filtered and 10 mL was titrated in order to determine excess base (using HCl) and excess acid (using NaOH), using Eq. (1), where *m* is the mass (g) of adsorbent, *V*_{0B} is the initial solution volume (L), *M*_T is the titrating solution concentration (mol L⁻¹), *V*_B is the titrating volume spent in the blank solution (L), and *V*_{al} is the sample volume used during the titrating process (L). The result *B*, given in mol L⁻¹, indicates the quantity of acidic and basic groups.

$$B = \frac{\left(\frac{V_{0B} \cdot M_T \cdot (V_B - V_{am})}{V_{al}} \right)}{m} \quad (1)$$

To investigate the adsorbent surface charge, the point of zero charge (pH_{pzc}) was determined, following an adapted method [25], in which a series of NaCl solutions were prepared and adjusted to different pH (2–12). Then, 0.02 g of adsorbent was added to each solution, and flasks were placed inside a TE-4200 orbital incubator shaker (Tecnal®), operating at 250 rpm and 298 K for 24 h. At the end, drift in pH was measured.

Surface area, pore-volume, and pore diameter of the adsorbent were determined using N₂ sorption/desorption analysis (NOVA 4000e – Quantachrome). Samples were previously treated in a vacuum system at 353 K during 3 h and 30 min, in order to remove all adsorbed contaminants, including water. Textural analysis was performed using as adsorbate nitrogen gas, and as refrigerating liquid, liquid nitrogen, through 20 adsorption and desorption points. Total analysis time was 4 h, using an interval of relative pressure (*p/p*⁰) between 0.04 and 1.0.

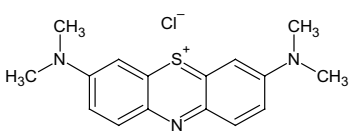
Scanning electron microscopy (SEM) (Carl-Zeiss EVO-15), equipped with an NTS BSD detector, was used to analyze surface morphology of MO husk.

2.2.2. Adsorption studies

Quantification of MB was performed using UV-Vis Spectrometry (UV5100 – Global Trade Technology) at 665 nm (λ_{max}). Batch experiments were performed at 298 K. In Erlenmeyer flasks containing 50 mL of a 25 mg L⁻¹ MB solution, 0.05 g of the adsorbent was added and shaken at 250 rpm. Aliquots were collected from each flask at given times and centrifuged for 10 min, and after that, analyzed to determine the residual MB concentration using UV-Vis spectroscopy. Standard curve was established over the range of 0.5–5 mg L⁻¹. All experiments were performed in triplicate, at pH 7.

Removal percentage (*R*) and adsorption capacity (*q*_t) were calculated by Eqs. (2) and (3), respectively, where *C*₀ and *C*_e are the initial and equilibrium MB concentration (mg L⁻¹),

Table 1
Physicochemical properties of MB [5,21]

Molecular structure	
Molecular formula	C ₁₆ H ₁₈ N ₃ SCl
Molecular weight	319.85 g mol ⁻¹
Solubility in water	43.21 g L ⁻¹ at 25°C
Maximum adsorption wavelength	665 nm
Uses	Dyeing of wood, cotton, and silk
Nature	Cationic dye

V is the volume of MB solution (L), m is the adsorbent mass (g), and q_t is the adsorption capacity (mg g^{-1}) [26].

$$R(\%) = \frac{(C_0 - C_e)}{C_0} \times 100 \quad (2)$$

$$q_t = \frac{(C_0 - C_e) \times V}{m} \quad (3)$$

2.2.3. Kinetics

Kinetic studies were performed taking aliquots at different times over 300 min. Adsorption kinetics were evaluated by applying pseudo-first- and pseudo-second-order, Elovich, Avrami, and intra-particle diffusion non-linear models (Table 2).

2.2.4. Isotherms

Isotherm evaluations were made by taking samples after equilibrium time, at 298 and 308 K. Langmuir, Freundlich, and Dubinin–Radushkevich models were used to evaluate adsorption isotherms (Table 3).

2.2.5. Thermodynamics

Adsorption experiments were conducted at 293, 298, 308, and 318 K to calculate the thermodynamic parameters ΔG° (Gibbs free energy of adsorption), ΔH° (enthalpy change), and ΔS° (entropy change). Gibbs free energy was obtained by Eq. (13), where ΔG° is the Gibbs free energy (J mol^{-1}), R is

Table 2
Pseudo-first-order, pseudo-second-order, intraparticle diffusion, Elovich, and Avrami kinetic models [26–29]

Model	Equation	Equation number
Pseudo-first-order	$q_t = q_e (1 - \exp(-k_1 \cdot t))$	Eq. (4)
Pseudo-second-order	$q_t = \frac{(q_e^2 \cdot k_2 \cdot t)}{(1 + k_2 \cdot q_e \cdot t)}$	Eq. (5)
Intraparticle diffusion	$q_t = k_{id} \cdot \sqrt{t} + C$	Eq. (6)
Elovich	$q_t = \frac{1}{\beta_E} \cdot \log(1 + \alpha_E \cdot \beta_E \cdot t)$	Eq. (7)
Avrami	$\alpha_A = 1 - \exp(-k_{av} \cdot t^{n_{av}})$	Eq. (8)

q_t and q_e are the amount of MB adsorbed at time t and at equilibrium, respectively (mg g^{-1}), k_1 and k_2 are the pseudo-first (min^{-1}) and pseudo-second-order rate constants ($\text{g mg}^{-1} \text{min}^{-1}$), respectively, k_{id} is the intraparticle diffusion constant ($\text{mg g}^{-1/2} \text{min}^{-1/2}$), C is the intercept of the straight line obtained from the plot of q_t vs. $t^{1/2}$, β_E and α_E are the desorption constant (g mg^{-1}) and initial adsorption constant of Elovich ($\text{mg g}^{-1} \text{min}^{-1}$), respectively, α_A represents q_t/q_e at time t (min^{-1}), k_{av} is the Avrami constant (min^{-1}), and n_{av} is the Avrami index.

Table 3
Langmuir, Freundlich, and Dubinin–Radushkevich isotherm models [26]

Model	Equation	Equation number
Langmuir	$q_e = \frac{q_{\max} K_L C_e}{1 + K_L C_e}$	Eq. (9)
Freundlich	$q_e = K_F C_e^{n_F}$	Eq. (10)
Dubinin–Radushkevich	$\log q = \log q_{DR} - k_{DR} \varepsilon^2$	Eq. (11)
	$\varepsilon^2 = RT \ln \left(1 + \frac{1}{C_e} \right)$	Eq. (12)

q_e is the equilibrium adsorption capacity (mg g^{-1}), q_{\max} is the maximum adsorption capacity (mg g^{-1}), K_L is the Langmuir constant (L mg^{-1}), C_e is the equilibrium concentration of MB (mg L^{-1}), K_F is the Freundlich constant (mg g^{-1}), n_F is the heterogeneity factor (dimensionless), ε is the Polanyi potential (kJ mol^{-1}), k_{DR} is the constant related to the adsorption energy ($\text{mol}^2 \text{kJ}^{-2}$), q_{DR} is the theoretical saturation capacity (mg g^{-1}), R is the universal gas constant ($8.314 \text{ J mol}^{-1} \text{ K}^{-1}$), T is the temperature (K).

the universal gas constant ($8.314 \text{ J mol}^{-1} \text{ K}^{-1}$), T is the temperature (K), and K_C is the thermodynamic equilibrium constant.

$$\Delta G^\circ = -RT \ln K_C \quad (13)$$

In order to accomplish a correlation between isothermal and thermodynamic parameters, adjustments are necessary. The Langmuir constant (K_L), given in L mg^{-1} , can be used to obtain K_L^0 , the standard equilibrium constant (dimensionless). Charged adsorbates, as methylene blue in certain pH conditions, can cause deviations between both values [30,31]. This adjustment can be expressed as described in Eq. (14) [31], where K_L^0 is the standard equilibrium constant, K_L is the Langmuir constant (L mg^{-1}), M is the molar mass (g mol^{-1}), 55.5 is the concentration of water (mol L^{-1}), and 10^3 is the term used to convert mg^{-1} to g^{-1} .

$$K_L^0 = K_L M \cdot (55.5 \cdot 10^3) \quad (14)$$

Therefore, K_L^0 is now dimensionless and can be used to calculate the other thermodynamic parameters as described in Eqs. (15) and (16).

$$\ln K_L^0 = \left(\frac{\Delta S^\circ}{R} \right) - \left(\frac{\Delta H^\circ}{RT} \right) \quad (15)$$

$$\Delta G^\circ = \Delta H - T \Delta S^\circ \quad (16)$$

3. Results and discussion

3.1. Characterization of the adsorbent

SEM images (Fig. 1) show that surface of MO is characterized by an extensive network of micro-pores,

corroborating results obtained with textural analysis, which indicated a high contribution of micropores (89.7%) to the total Brunauer–Emmett–Teller (BET) surface area.

BET surface area, microporous area, average pore volume, and pore diameter were equal to $318.4 \text{ m}^2 \text{ g}^{-1}$, $285.6 \text{ m}^2 \text{ g}^{-1}$, $0.1774 \text{ cm}^3 \text{ g}^{-1}$, and 1.08 nm , respectively. Alongside porosity, surface functional groups have a crucial role in the adsorption process efficiency [32]. Boehm titration is commonly used to determine these groups on activated carbons [33]. Nevertheless, this method can also be used for bio-sorbents [34]. Boehm's titration revealed low concentrations of basic groups (pyrones) and acid ligands (carboxylic and lactonic groups). Carboxylate anions can interact with nitrogen if the latter is positively charged in methylene blue, while the oxygen of pyrone's carbonyl can act as an electron donor and the aromatic ring of the dye as an electron receptor [35–37]. These interactions between adsorbate and adsorbent highlight the role of superficial ligands in adsorption.

Concurrently with Boehm titration, Fourier-transform infrared spectroscopy (FTIR) analysis was considered in this study to evaluate functional groups. FTIR spectrums of MO seed husks before and after adsorption are displayed in Fig. 2a.

The broad peak near $3,300 \text{ cm}^{-1}$ can be associated with the presence of hydroxyl groups from protein and fatty acid structures, as well as to N–H ligand, also from proteins, or

silane groups (SiOH) [38]. Lignocellulosic materials have high contents of hydroxyl groups and other reaction sites capable to promote substitution reaction with metal ions to form complexes in solution via donation of electron pairs [39,40]. These functional groups can dissociate and participate in sorption processes through interactions such as electrostatic, hydrogen bonding, and van der Waals forces, interacting with charged dyes, as methylene blue, in certain physicochemical conditions [1]. Peaks at $2,923$ and $2,854 \text{ cm}^{-1}$ can be caused by C–H stretching vibrations of methylene groups and may be due to the presence of fatty acids [41]. The sharp peak at $1,647 \text{ cm}^{-1}$ can be attributed to the carbonyl group of amides. After adsorption, peaks at 883 and $1,599 \text{ cm}^{-1}$ emerged, which represents C–H bending in the heterocyclic aromatic ring and vibrations of the C=C and C=N bonds in the heterocycle, respectively [42–44]. These changes substantiate the occurrence of adsorption of MB onto MO husk. FTIR spectrum of MB can be seen in Fig. 2b.

In order to evaluate the surface charge of MO seed husks, pH_{PZC} was determined, as displayed in Fig. 3.

It was established a value equal to 5.1 ± 0.3 , obtained from the graphic point where ΔpH is zero. This parameter indicates that MO seed husks surface will be carried with positive charges in pH lower than 5.1, and with negative charges in pH higher than 5.1. As all adsorption experiments were performed at $\text{pH} = 7$, MO surface was mainly negative charged

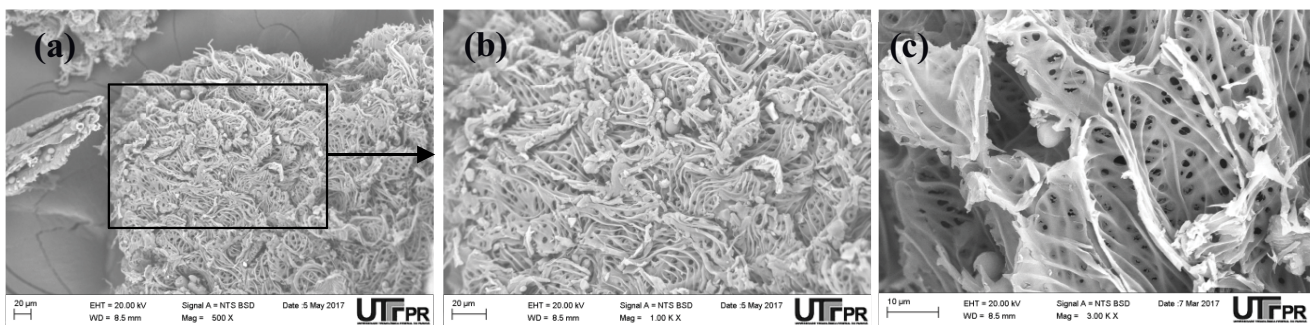


Fig. 1. SEM images of MO under (a) 500, (b) 1,000, and (c) 3,000 magnification.

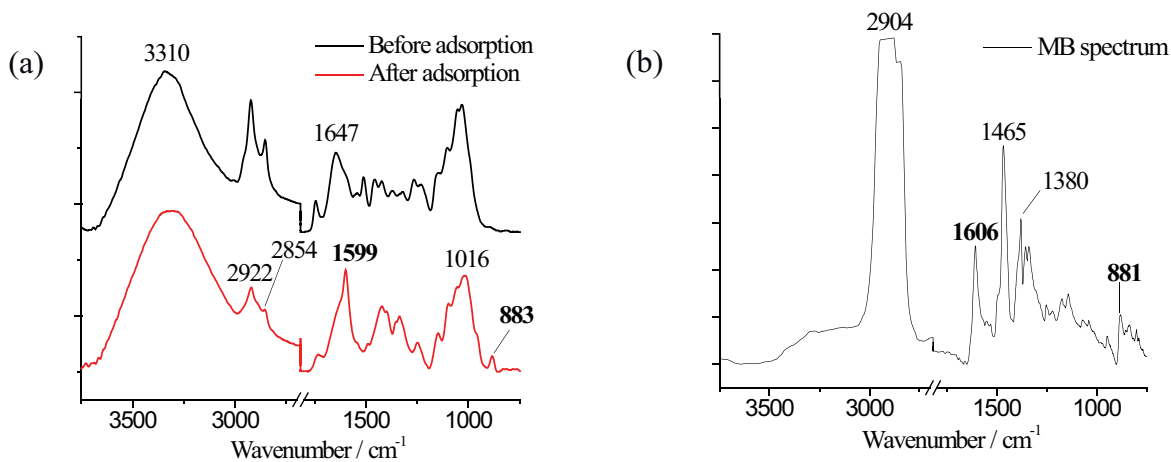


Fig. 2. FTIR spectrum of MO seed husk (a) before and after adsorption and (b) FTIR spectrum of MB.

in this condition, being advantageous to remove a cationic dye as MB.

3.2. Methylene blue adsorption

3.2.1. Kinetic modeling

All kinetic studies were conducted at 298 K. The pseudo-first and pseudo-second kinetic adsorption curves are shown in Fig. 4.

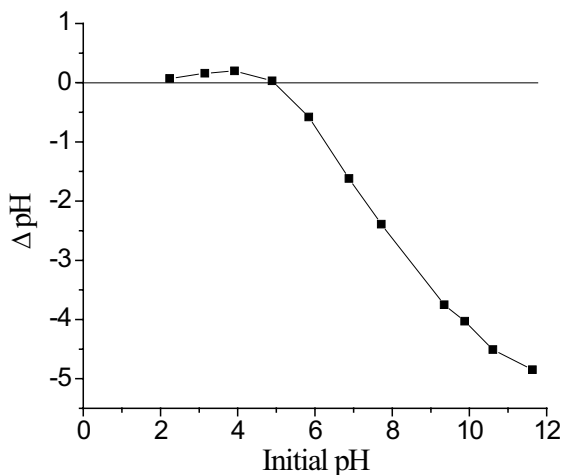


Fig. 3. Point of zero charge (pH_{pzc}) of MO seed husks.

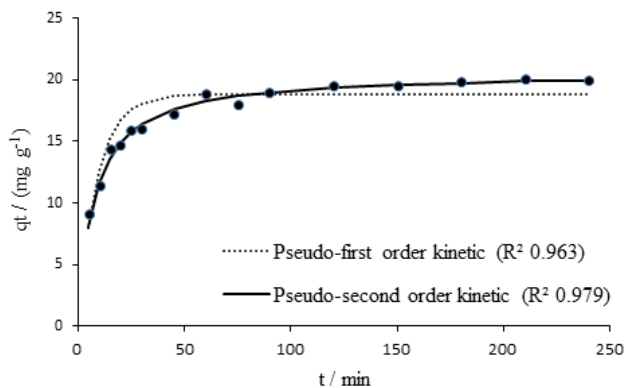


Fig. 4. Pseudo-first- and pseudo-second-order sorption kinetics plots of MB onto MO seed husk at 298 K (MB concentration: 25 mg L^{-1}).

Table 4

Pseudo-first- and pseudo-second-order model parameters for adsorption of methylene blue on MO seed husks (MB concentration: 25 mg L^{-1})

Pseudo-first-order			Pseudo-second-order		
q_e	k_1	R^2	q_e	k_2	R^2
18.8 ± 0.2	0.11 ± 0.06	0.963	20.6 ± 0.2	0.0063 ± 0.0004	0.979

q_e is the equilibrium adsorption capacity (mg g^{-1}), k_1 is the pseudo-first-order rate constant (min^{-1}), k_2 is the pseudo-second-order rate constant ($\text{g mg}^{-1} \text{min}^{-1}$).

Kinetic parameters were calculated and are listed in Table 4.

Pseudo-first- and pseudo-second-order equations, also known as Lagergren and Blanchard model, respectively, try to represent all steps of the adsorptive process, including film diffusion, internal particle diffusion, and adsorption [45]. The application of pseudo-first- and pseudo-second-order models provided an excellent adjustment to experimental data, with R^2 equal to 0.963 and 0.979, respectively. Thus, it was found that the pseudo-second-order model was the best of both models evaluated, and equilibrium was achieved in 90 min.

Nonetheless, adsorption and desorption in porous adsorbents are not determined only by superficial and general sorption, but by diffusion processes as well [46]. Intraparticle diffusion is known as one of the most important controlling steps in adsorptive processes, and its contribution needs to be considered in kinetic studies [26]. Weber and Morris tried to equate the contribution of intraparticle diffusion (Eq. (6)), whereas Elovich attempted to describe a general diffusion process. Parameters in the Elovich model can also be used to evaluate the potential contribution of chemisorption during adsorption (Eq. (7)) [26,27]. Likewise, Avrami tried to evaluate adsorption by developing a model which represents a multi-step process, without taking into account the interaction mechanisms between adsorbate and adsorbent (Eq. (8)) [28,29].

In order to draw more conclusions about the adsorption process, Webber–Morris, Avrami, and Elovich kinetic models were also applied to experimental data. The first set of analyses confirmed the impact of multiple mechanisms in adsorption. Intraparticle diffusion (Webber–Morris) plot (Fig. 5) displayed two linear segments, each of them indicating one step during adsorption.

The first portion describes the effect of external surface in adsorption, due to liquid film diffusion or electrostatic attraction between superficial charges and the dye structure ($R^2 = 0.918$). The second portion demonstrates gradual adsorption by intraparticle diffusion ($R^2 = 0.928$), as reported by other researchers who worked with methylene blue [9,47] and multiple dyes [48].

Although a new segment was observed after 210 min ($t^{0.5} = 14.50 \text{ min}^{0.5}$) (Fig. 5), experimental data was not enough to propose the existence of another step of adsorption. Weber–Morris model with three line segments has a final step which indicates that the remaining concentration may be insufficient to undergo a diffusion process [48,49]. Parameters of the Intraparticle diffusion (Weber–Morris) kinetic model are depicted in Table 5.

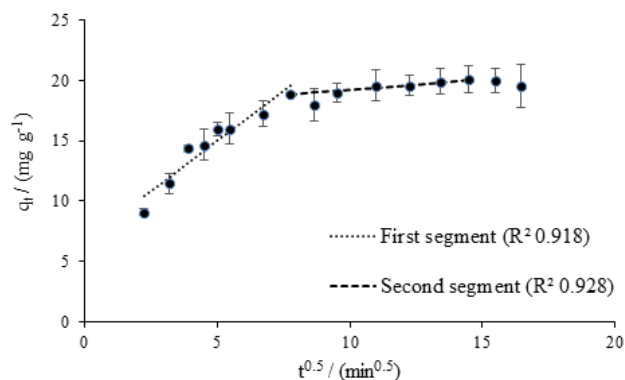


Fig. 5. Intraparticle diffusion kinetic modeling for the adsorption of MB onto MO seed husks.

Table 5
Intraparticle diffusion kinetic model parameters for adsorption of MB onto MO seed husk (MB concentration: 25 mg L⁻¹)

First segment			Second segment		
k_{id1}	C_1	R^2	k_{id2}	C_2	R^2
1.66	6.68	0.918	0.17	17.58	0.928

k_{id1} is the intraparticle diffusion constant of the first segment ($\text{mg g}^{-1/2} \text{min}^{-1/2}$), k_{id2} is the intraparticle diffusion constant of the second segment ($\text{mg g}^{-1/2} \text{min}^{-1/2}$), C_1 is the intercept of the straight line obtained from the plot of q_t vs. $t^{1/2}$ of first segment (mg g^{-1}), and C_2 is the intercept of the straight line obtained from the plot of q_t vs. $t^{1/2}$ of the second segment (mg g^{-1}).

Table 6
Avrami and Elovich kinetic model parameters for adsorption of MB onto MO seed husks (MB concentration: 25 mg L⁻¹)

Avrami			Elovich		
n_{av}	k_{av}	R^2	α_E	β_E	R^2
0.59	0.24	0.985	22.47	0.35	0.940

n_{av} is the Avrami index, k_{av} is the Avrami constant (min^{-1}), α_E is the initial adsorption constant of Elovich ($\text{mg g}^{-1} \text{min}^{-1}$), β_E is the desorption constant of Elovich (g mg^{-1}).

Since C_1 is different than zero, it is assumed that intraparticle diffusion is not the rate-limiting step, and other mechanisms could be also responsible for adsorption. In another study, researchers believed that methylene blue could not be fully interpreted by Weber–Morris, since this model is most suitable for molecules with similar sizes to micro and macro-pores [50]. In the case of MB, with a typical size to keep adsorption going through mesopores, intraparticle diffusion is not favored [51].

In order to express the kinetic characteristics related to multistep adsorption, the Avrami model was fitted to the experimental data (Table 6).

The adsorption was well-described by the Avrami model, with a determination coefficient of 0.985. The value of n_{av} demonstrated that the adsorption process might not be limited by surface reaction ($n_{av} < 1$), and the fractional-order indicates that the reaction occurred in multi pathways [52,53].

Adsorption heterogeneity was also evaluated using Elovich equations. The good representation of experimental data by this model showed that the effects of desorption and interaction between adsorbates already adsorbed was not significant to adsorption [54]. Also, as it can be seen in Table 6, values of α_E higher than β_E indicate that the adsorbate prefers to interact with MO husk rather than returning to an aqueous solution. This interaction may occur through chemisorption with rate-determining steps involving electron exchange [55].

3.2.2. Adsorption isotherms

The Langmuir model was developed with the conception of monolayer surface coverage, where limited adsorption sites would be homogeneous, adsorbing one single molecule of adsorbate, with no interaction among the adsorbed molecule and between other sites [56–58]. Nonetheless, the Freundlich model describes an exponential distribution of active sites and their energies in heterogeneous surfaces, no more restricted to monolayer coverage [59,60]. Dubinin and Radushkevich found that it was possible to relate the adsorptive mechanism with thermodynamic considerations using the Polanyi adsorption potential. The model proposed by them uses thermodynamic parameters to evaluate the transfer of adsorbate onto the heterogeneous surface of the adsorbent and can be described as a Gaussian energy distribution [61–63]. Fig. 6 shows the adsorption of MB at 298 and 308 K as a function of C_e , fitted to Langmuir and Freundlich isotherm model.

Parameters of Langmuir and Freundlich are described in Table 7.

The experimental data were better correlated with Langmuir ($R^2 = 0.960$ and 0.986). The essential characteristic of the isotherm was expressed by the heterogeneity factor (n_F), equal to 0.61 and 0.73, which revealed favorable adsorption. Through these experiments, it is apparent that temperature has a positive influence on q_{max} , and it represented an increase in active sites in the adsorbent. Also, K_L and K_F decreased, which could represent a reduction in interactions between adsorbent and adsorbate. Adsorption of tartrazine with MO seed also occurred with a decrease in K_F [18]. Therefore, adsorption of methylene blue onto MO husk can be declared as temperature-sensitive, since experimental data showed that increasing it may have a positive effect on attractive forces between solid and solute, decreasing viscosity of the solvent and enhancing the solubility rate and mobility of the adsorbate [6,64,65].

Experimental adsorption isotherm was also fitted to Dubinin–Radushkevich model (Table 8).

The correlation coefficient ($R^2 = 0.948$) confirmed the good fit of experimental results on this theoretical model. In general, removal of dyes by adsorbent materials can assume four steps: (1) migration of dye from solution to adsorbent surface, (2) diffusion through the limit layer, (3) intraparticle diffusion, and (4) chemical reaction on active sites due to ion-exchange or complexation [26,28]. The mean free energy (E_c) given by Dubinin–Radushkevich model indicates if adsorption involves primarily ion-exchange ($8\text{--}16 \text{ kJ mol}^{-1}$) or physical adsorption ($E_c < 8 \text{ kJ mol}^{-1}$) [66]. The mean free energy (E_c) was 9.13 kJ mol^{-1} , and based on

Table 7
Langmuir and Freundlich isotherms parameters for adsorption of MB onto MO seed husks at 298 and 308 K

T	Langmuir			Freundlich		
	q_{\max}	K_L	R^2	$K_F (10^{-2})$	n_F	R^2
298	69.73	9.06	0.960	7.66	0.61	0.910
308	88.20	4.52	0.986	4.92	0.73	0.966

T is the temperature (K), q_{\max} is the maximum monolayer adsorption capacity (mg g^{-1}), K_L is the Langmuir constant (L mg^{-1}), K_F is the Freundlich constant (mg g^{-1}), n_F is the heterogeneity factor (dimensionless).

Table 8
Dubinin–Radushkevich isotherm parameters for adsorption of methylene blue onto MO seed husks

q_{DR}	k_{DR}	E_c	R^2
0.001	6.0×10^{-9}	9.13	0.948

q_{DR} is the theoretical saturation capacity (mg g^{-1}), k_{DR} is the constant related to the adsorption energy ($\text{mol}^2 \text{J}^{-2}$), E_c is the mean free energy (kJ mol^{-1}).

Table 9
Values of q_{\max} found in the literature for removal of MB

Adsorbent	$q_{\max} (\text{mg g}^{-1})$	Reference
Activated carbon from waste carpets	769.20	[67]
Arginine modified activated carbon	219.90	[5]
Brown macroalga	95.45	[68]
MO seed husk	69.73	Present study
<i>Paspalum maritimum</i>	56.18	[69]
Yellow passion fruit waste	44.70	[70]

this result, the ion-exchange mechanism might be predicted as an important step in methylene blue adsorption.

A comparison with the results of q_{\max} found in literature can be seen in Table 9.

Although values of q_{\max} are superior in some studies, the time required to the system to reach equilibrium can be superior also. When removing MB using brown macroalga, sorption was carried out during 120 min [68], and when employing activated carbons made from waste carpets, 12 h were necessary [67]. In the present study, 90 min were sufficient for equilibrium to be established.

3.2.3. Thermodynamic study

Adsorption studies were carried out at various temperatures: 293, 298, 308, and 318 K. The standard Gibbs free energy (ΔG°) is related to the spontaneity of the process, the standard enthalpy (ΔH°) is dependent on interaction between adsorbate and adsorbent, while the standard entropy (ΔS°) is associated with the degree of disorder of this system [71]. Thermodynamic parameters were

Table 10
Thermodynamic parameters of MB adsorption in seed husks of MO

T (K)	$K_L^0 (10^6)$	ΔG°	ΔH°	ΔS°	R^2
293	1.6086	-0.170	-98.84	-0.21	0.831
298	1.6088	-0.173			
308	0.8024	-0.188			
318	0.0617	-0.240			

T is the temperature (K), K_L^0 is the standard equilibrium constant (dimensionless), ΔG° is the Gibbs free energy (kJ mol^{-1}), ΔH° is the enthalpy change (kJ mol^{-1}), ΔS° is the entropy change ($\text{kJ mol}^{-1} \text{K}^{-1}$).

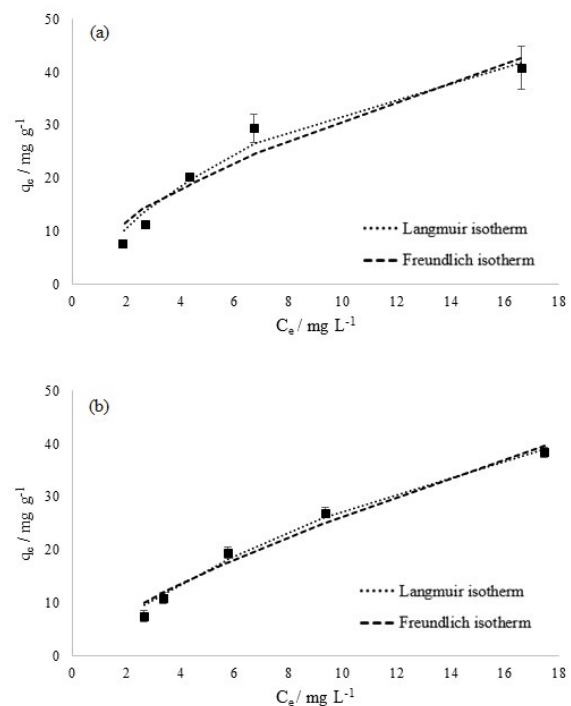


Fig. 6. Equilibrium isotherm fitted to Langmuir and Freundlich models for MB adsorption onto MO seed husks at 298 K (a) and 308 K (b).

calculated according to Eqs. (13) and (14), and their values are given in Table 10.

A decrease in adsorption capacity (q_e) with increasing temperature was observed, as shown in Fig. 6. In addition, the value of ΔH° ($-98.84 \text{ kJ mol}^{-1}$) indicates an exothermic process, typical of chemical adsorption mechanisms such as bond formation, ligand exchange (substitution) or charge-transfer reactions [72].

Compared to the results of Langmuir and Freundlich isotherms, values obtained from Gibbs free energy demonstrate that an increase in temperature enhances mobility of adsorbate in solution, growing its affinity with the adsorbent. However, it is not possible to exclude the possibility of desorption affecting the adsorption capacity, as (K_L) and (K_F) decreased with temperature. The negative values of Gibbs free energy also suggest that adsorption of methylene blue

was spontaneous, enthalpy-driven, and accompanied by a decrease in entropy, indicating that the adsorption promoted no changes in the internal structure of the adsorbent. It also indicates a reduction in disorder and randomness of the system at different temperature conditions [73]. The same behavior was observed in previous experiments described in the literature, as in the adsorption of methylene blue onto lignocellulosic materials [1], chitosan-based materials [73], and activated carbons produced from waste carpets [67].

4. Conclusion

Methylene blue removal by adsorption onto MO seed husks was found to be a promising technology due to low costs, simple preparation of the adsorbent and high adsorption capacity (69.73 mg g^{-1}) achieved with this material. The sorption data of MB onto MO seed husks was well-fitted by Avrami kinetic model and best described by Langmuir isotherm. Ion-exchange was proposed to be a mechanism that can contribute to the adsorption with a great role in the multi-step adsorptive process, supported by kinetic evaluations, FTIR results, and Dubinin–Radushkevich isotherm. Thermodynamic parameters demonstrated that adsorption was exothermic, spontaneous, and enthalpy-driven, which agrees with other studies of methylene blue adsorption. MO seed husks, a material normally discarded, can be a source of income in poor countries and, at the same time, improve water quality for the local population.

Acknowledgments

The authors would like to acknowledge the Multi-User Center for Materials Characterization (CMCM) – UTFPR by the support in SEM analysis, Soil Mineralogy Laboratory (LMS) – UFPR for helping with textural analysis, and the Multi-User Chemical Analysis Laboratory (LAMAQ) – UTFPR for providing assistance with FTIR analysis. This work was supported by the National Council for Scientific and Technological Development (CNPq).

References

- [1] S. Manna, D. Roy, P. Saha, D. Gopakumar, S. Thomas, Rapid methylene blue adsorption using modified lignocellulosic materials, *Process Saf. Environ. Prot.*, 107 (2017) 346–356.
- [2] J.A. González, M.E. Villanueva, L.L. Piehl, G.J. Copello, Development of a chitin/graphene oxide hybrid composite for the removal of pollutant dyes: adsorption and desorption study, *Chem. Eng. J.*, 280 (2015) 41–48.
- [3] K.N. Aboua, Y.A. Yobouet, K.B. Yao, D.L. Goné, A. Trokourey, Investigation of dye adsorption onto activated carbon from the shells of Macoré fruit, *J. Environ. Manage.*, 156 (2015) 10–14.
- [4] F. Nekouei, S. Nekouei, I. Tyagi, V.K. Gupta, Kinetic, thermodynamic and isotherm studies for acid blue 129 removal from liquids using copper oxide nanoparticle-modified activated carbon as a novel adsorbent, *J. Mol. Liq.*, 201 (2015) 124–133.
- [5] M. Naushad, A.A. Alqadami, Z.A. AlOthman, I.H. Alsohaimi, M.S. Algamdi, A.M. Aldawsari, Adsorption kinetics, isotherm and reusability studies for the removal of cationic dye from aqueous medium using arginine modified activated carbon, *J. Mol. Liq.*, 293 (2019) 111442.
- [6] M.J. Ahmed, Application of agricultural based activated carbons by microwave and conventional activations for basic dye adsorption: review, *J. Environ. Chem. Eng.*, 4 (2016) 89–99.
- [7] P. Staron, J. Chwastowski, M. Banach, Sorption behavior of methylene blue from aqueous solution by raphia fibers, *Int. J. Environ. Sci. Technol.*, 16 (2019) 8449–8460.
- [8] S.H. Chen, A.S.Y. Ting, Biodecolorization and biodegradation potential of recalcitrant triphenylmethane dyes by *Corioliopsis* sp. isolated from compost, *J. Environ. Manage.*, 150 (2015) 274–280.
- [9] Q. Li, Y. Li, X. Ma, Q. Du, K. Sui, D. Wang, C. Wang, H. Li, Y. Xia, Filtration and adsorption properties of porous calcium alginate membrane for methylene blue removal from water, *Chem. Eng. J.*, 316 (2017) 623–630.
- [10] F. Marrakchi, M.J. Ahmed, W.A. Khanday, M. Asif, B.H. Hameed, Mesoporous-activated carbon prepared from chitosan flakes via single-step sodium hydroxide activation for the adsorption of methylene blue, *Int. J. Biol. Macromol.*, 98 (2017) 233–239.
- [11] A. Delelegn, S. Sahile, A. Husen, Water purification and antibacterial efficacy of *Moringa oleifera* Lam, *Agric. Food Secur.*, 7 (2018) 1–10.
- [12] M.E.A. El-Hack, M. Alagawany, A.S. Elrys, E.S.M. Desoky, H.M.N. Tolba, A.S.M. Elnahal, S.S. Elnesr, A. Swelum, Effect of forage *Moringa oleifera* L. (moringa) on animal health and nutrition and its beneficial applications in soil, plants and water purification, *Agriculture*, 8 (2018) 1–22.
- [13] L.L.S. Gámez, M.L.D. Risco, R.E.S. Cano, Comparative study between *M. oleifera* and aluminum sulfate for water treatment: case study Colombia, *Environ. Monit. Assess.*, 187 (2015) 1–9.
- [14] A.K. Virk, C. Kumari, A. Tripathi, A. Kakade, X. Li, S. Kulshrestha, Development and efficacy analysis of a *Moringa oleifera* based potable water purification kit, *J. Water Process Eng.*, 27 (2019) 37–46.
- [15] R.M. Paixão, I.M. Reck, R.G. Gomes, R. Bergamasco, M.F. Vieira, A.M.S. Vieira, Water decontamination containing nitrate using biosorption with *Moringa oleifera* in dynamic mode, *Environ. Sci. Pollut. Res. Int.*, 25 (2018) 21544–21554.
- [16] M. Matouq, N. Jildeh, M. Qtaishat, M. Hindiyeh, M.Q. Al Syouf, The adsorption kinetics and modeling for heavy metals removal from wastewater by *Moringa* pods, *J. Environ. Chem. Eng.*, 3 (2015) 775–784.
- [17] C.O. Bezerra, L.F. Cusioli, H.B. Quesada, L. Nishi, D. Mantovani, M.F. Vieira, R. Bergamasco, Assessment of the use of *Moringa oleifera* seed husks for removal of pesticide diuron from contaminated water, *Environ. Technol.*, 41 (2020) 191–201.
- [18] I.M. Reck, R.M. Paixão, R. Bergamasco, M.F. Vieira, A.M.S. Vieira, Removal of tartrazine from aqueous solutions using adsorbents based on activated carbon and *Moringa oleifera* seeds, *J. Cleaner Prod.*, 171 (2018) 85–97.
- [19] S.N. Do Carmo, F.Q. Damásio, V.N. Alves, T.L. Marques, N.M.M. Coelho, Direct determination of copper in gasoline by flame atomic absorption spectrometry after sorption and preconcentration on *Moringa oleifera* husk, *Microchem. J.*, 110 (2013) 320–325.
- [20] J.A.N. Oliveira, L.M.C. Siqueira, J.A.S. Neto, N.M.M. Coelho, V.N. Alves, Preconcentration system for determination of lead in chicken feed using *Moringa oleifera* husks as a biosorbent, *Microchem. J.*, 133 (2017) 327–332.
- [21] A. Salimi, A. Roosta, Experimental solubility and thermodynamic aspects of methylene blue in different solvents, *Thermochim. Acta*, 675 (2019) 134–139.
- [22] ASTM INTERNATIONAL, ASTM D2862–10: Standard Test Method for Particle Size Distribution of Granular Activated Carbon, West Conshohocken, 2010.
- [23] H.P. Boehm, Surface oxides on carbon and their analysis: a critical assessment, *Carbon*, 40 (2002) 145–149.
- [24] H.P. Boehm, Some aspects of the surface chemistry of carbon blacks and other carbons, *Carbon*, 32 (1994) 759–769.
- [25] L. Ramrakhiani, A. Halder, A. Majumder, A.K. Mandal, S. Majumdar, S. Ghosh, Industrial waste derived biosorbent for toxic metal remediation: mechanism studies and spent biosorbent management, *Chem. Eng. J.*, 308 (2017) 1048–1064.
- [26] H.N. Tran, S.J. You, A. Hosseini-Bandegharai, H.P. Chao, Mistakes and inconsistencies regarding adsorption of contaminants from aqueous solutions: a critical review, *Water Res.*, 120 (2017) 88–116.

- [27] H.I. Inyang, A. Onwawoma, S. Bae, The Elovich equation as a predictor of lead and cadmium sorption rates on contaminant barrier minerals, *Soil Tillage Res.*, 155 (2016) 124–132.
- [28] G. Crini, P. Badot, Application of chitosan, a natural aminopolysaccharide, for dye removal from aqueous solutions by adsorption processes using batch studies: a review of recent literature, *Prog. Polym. Sci.*, 33 (2008) 399–347.
- [29] A.R. Cestari, E.F. Vieira, A.A. Pinto, E.C. Lopes, Multistep adsorption of anionic dyes on silica/chitosan hybrid: 1. Comparative kinetic data from liquid- and solid-phase models, *J. Colloid Interface Sci.*, 292 (2005) 363–372.
- [30] S.K. Milonjic, A consideration of the correct calculation of thermodynamic parameters of adsorption, *J. Serb. Chem. Soc.*, 72 (2007) 1363–1367.
- [31] X. Zhou, The unit problem in the thermodynamic calculation of adsorption using the Langmuir equation, *Chem. Eng. Commun.*, 201 (2014) 1459–1467.
- [32] W. Shen, Z. Li, Y. Liu, Surface chemical functional groups modification of porous carbon, *Recent Pat. Chem. Eng.*, 1 (2008) 27–40.
- [33] J. Schönherr, J.R. Buchheim, P. Scholz, P. Adelhelm, Boehm titration revisited (Part II): a comparison of Boehm titration with other analytical techniques on the quantification of oxygen-containing surface groups for a variety of carbon materials, *C. J. Carbon Res.*, 4 (2018) 1–16.
- [34] M. Farnane, H. Tounsadi, R. Elmoubarki, F.Z. Mahjoubi, A. Elhalil, S. Saqrane, M. Abdennouri, S. Qourzal, N. Barka, Alkaline treated carob shells as sustainable biosorbent for clean recovery of heavy metals: kinetics, equilibrium, ions interference and process optimization, *Ecol. Eng.*, 101 (2017) 9–20.
- [35] M.A. Montes-Morán, D. Suárez, J.A. Menéndez, E. Fuente, On the nature of basic sites on carbon surfaces: an overview, *Carbon*, 42 (2004) 1219–1225.
- [36] C. Moreno-Castilla, Adsorption of organic molecules from aqueous solutions on carbon materials, *Carbon*, 42 (2004) 83–94.
- [37] A.M.M. Vargas, A.L. Cazetta, M.H. Kunita, T.L. Silva, V.C. Almeida, Adsorption of methylene blue on activated carbon produced from flamboyant pods (*Delonix regia*): study of adsorption isotherms and kinetic models, *Chem. Eng. J.*, 168 (2011) 722–720.
- [38] V.N. Alves, S.O. Borges, N.M.M. Coelho, Direct zinc determination in Brazilian sugar cane spirit by solid-phase extraction using *Moringa oleifera* husks in a flow system with determination by FAAS, *Int. J. Anal. Chem.*, 2011 (2011) 1–8.
- [39] D.N.S. Hon, *Chemical Modification of Lignocellulosic Materials*, Routledge, New York, NY, 1996.
- [40] T.A.H. Nguyen, H.H. Ngo, W.S. Guo, J. Zhang, S. Liang, Q.Y. Yue, Q. Li, T.V. Nguyen, Applicability of agricultural waste and by-products for adsorptive removal of heavy metals from wastewater, *Bioresour. Technol.*, 148 (2013) 574–585.
- [41] V.N. Alves, N.M.M. Coelho, Selective extraction and preconcentration of chromium using *Moringa oleifera* husks as biosorbent and flame atomic absorption spectrometry, *Microchem. J.*, 109 (2013) 16–22.
- [42] U. Chakraborty, T. Singha, R.R. Chianelli, C. Hansda, P.K. Paul, Organic-inorganic hybrid layer-by-layer electrostatic self-assembled film of cationic dye methylene blue and a clay mineral: spectroscopic and atomic force microscopic investigations, *J. Lumin.*, 187 (2017) 322–332.
- [43] A.A. Sari, F. Amriani, M. Muryanto, E. Triwulandari, Y. Sudiyan, V. Barlianti, P.D.N. Lotulung, T. Hadibarata, Mechanism, adsorption kinetics and applications of carbonaceous adsorbents derived from black liquor sludge, *J. Taiwan Inst. Chem. Eng.*, 77 (2017) 236–243.
- [44] O.V. Ovchinnikov, A.V. Evtukhova, T.S. Kondratenko, M.S. Smirnov, V.Y. Khokhlov, O.V. Erina, Manifestation of intermolecular interactions in FTIR spectra of methylene blue molecules, *Vib. Spectrosc.*, 86 (2016) 181–189.
- [45] M. Chang, R. Juang, Equilibrium and kinetic studies on the adsorption of surfactant, organic acids and dyes from water onto natural biopolymers, *Colloids Surf., A*, 269 (2005) 35–46.
- [46] C. Yao, T. Chen, A film-diffusion-based adsorption kinetic equation and its application, *Chem. Eng. Res. Des.*, 119 (2017) 87–92.
- [47] Z. Ezzeddine, I. Batonneau-Gener, Y. Pouilloux, H. Hamad, Removal of methylene blue by mesoporous CMK-3: kinetics, isotherms and thermodynamics, *J. Mol. Liq.*, 223 (2016) 763–770.
- [48] L. Eskandarian, M. Arami, E. Pajootan, Evaluation of adsorption characteristics of multiwalled carbon nanotubes modified by a poly(propylene imine) dendrimer in single and multiple dye solutions: isotherms, kinetics, and thermodynamics, *J. Chem. Eng. Data*, 59 (2014) 444–454.
- [49] B. Royer, N.F. Cardoso, E.C. Lima, J.C.P. Vagheti, N.M. Simon, T. Calvete, R.C. Veses, Applications of Brazilian pine-fruit shell in natural and carbonized forms as adsorbents to removal of methylene blue from aqueous solutions – kinetic and equilibrium study, *J. Hazard. Mater.*, 164 (2009) 1213–1222.
- [50] H. Karaer, I. Kaya, Synthesis, characterization of magnetic chitosan/active charcoal composite and using at the adsorption of methylene blue and reactive blue 4, *Microporous Mesoporous Mater.*, 232 (2016) 26–38.
- [51] A. Aygün, S. Yenisoay-Karakaş, I. Duman, Production of granular activated carbon from fruit stones and nutshells and evaluation of their physical, chemical and adsorption properties, *Microporous Mesoporous Mater.*, 66 (2003) 189–195.
- [52] N.F. Cardoso, E.C. Lima, T. Calvete, I.S. Pinto, C.V. Amavisca, T.H.M. Fernandes, R.B. Pinto, W.S. Alencar, Application of aqai stalks as biosorbents for the removal of the dyes reactive black 5 and reactive orange 16 from aqueous solution, *J. Chem. Eng. Data*, 56 (2011) 1857–1868.
- [53] R. George, S. Sugunan, Kinetics of adsorption of lipase onto different mesoporous materials: evaluation of Avrami model and leaching studies, *J. Mol. Catal. B: Enzym.*, 105 (2014) 26–32.
- [54] O. Pezoti Junior, A.L. Cazetta, R.C. Gomes, E.O. Barizão, I.P.A.F. Souza, A.C. Martins, T. Asefa, V.C. Almeida, Synthesis of ZnCl₂-activated carbon from macadamia nut endocarp (*Macadamia integrifolia*) by microwave-assisted pyrolysis: optimization using RSM and methylene blue adsorption, *J. Anal. Appl. Pyrolysis*, 105 (2014) 166–176.
- [55] P.D. Pathak, S.A. Mandavgane, B.D. Kulkarni, Fruit peel waste as a novel low-cost bio adsorbent, *Rev. Chem. Eng.*, 31 (2015) 361–381.
- [56] I. Langmuir, The adsorption of gases on plane surfaces of glass, 1707 mica and platinum, *J. Am. Chem. Soc.*, 40 (1918) 1361–1403.
- [57] J. Guo, Z. Zhai, L. Wang, Z. Wang, J. Wu, B. Zhang, J. Zhang, Dynamic and thermodynamic mechanisms of TFA adsorption by particulate matter, *Environ. Pollut.*, 225 (2017) 175–183.
- [58] D.M. Ruthven, *Principles of Adsorption and Adsorption Processes*, John Wiley & Sons, New York, NY, 1984.
- [59] E.J. Bottani, J.M.D. Tascón, *Adsorption by Carbons*, 1st ed., Elsevier, 2011.
- [60] N. Ayawei, A.N. Ebelegi, D. Wankasi, Modelling and interpretation of adsorption isotherms, *J. Chem.*, 2017 (2017) 1–11.
- [61] T.J. Bandoz, *Activated Carbon Surfaces in Environmental Remediation*, Academic Press, New York, NY, 2006.
- [62] M. Greenbank, M. Manes, Application of the Polanyi adsorption potential theory to adsorption from solution on activated carbon: adsorption of organic liquid mixtures from water solution, *J. Phys. Chem.*, 85 (1981) 3050–3059.
- [63] K.Y. Foo, B.H. Hameed, Insights into the modeling of adsorption isotherm systems, *Chem. Eng. J.*, 156 (2010) 2–10.
- [64] S. Afroz, T.K. Sen, M. Ang, H. Nishioka, Adsorption of methylene blue dye from aqueous solution by novel biomass *Eucalyptus sheathiana* bark: equilibrium, kinetics, thermodynamics and mechanism, *Desal. Water Treat.*, 57 (2016) 5858–5878.
- [65] P.Y.R. Suzuki, M.T. Munaro, C.C. Triques, S.J. Kleinübing, M.R.F. Klen, L.M.M. Jorge, R. Bergamasco, Biosorption of binary heavy metal systems: phenomenological mathematical modeling, *Chem. Eng. J.*, 313 (2017) 364–373.
- [66] A. Baldermann, A.C. Griebbacher, C. Baldermann, B. Purgstaller, I. Letofsky-Papst, S. Kaufhold, M. Dietzel, Removal of barium, cobalt, strontium, and zinc from solution by natural and synthetic allophone adsorbents, *Geosciences*, 8 (2018) 1–22.

- [67] A.F. Hassan, H. Elhadidy, Production of activated carbons from waste carpets and its application in methylene blue adsorption: kinetic and thermodynamic studies, *J. Environ. Chem. Eng.*, 5 (2017) 955–963.
- [68] E. Daneshvar, A. Vazirzadeh, A. Niazi, M. Kousha, M. Naushad, A. Bhatnagar, Desorption of methylene blue dye from brown macroalga: effects of operating parameters, isotherm study and kinetic modeling, *J. Cleaner Prod.*, 152 (2017) 443–453.
- [69] F. Silva, L. Nascimento, M. Brito, K. Silva, W.P. Junior, R. Fujiyama, Biosorption of methylene blue dye using natural biosorbents made from weeds, *Materials (Basel)*, 12 (2019) 1–16.
- [70] F.A. Pavan, E.C. Lima, S.L.P. Dias, A.C. Mazzoto, Methylene blue biosorption from aqueous solutions by yellow passion fruit waste, *J. Hazard. Mater.*, 150 (2008) 703–712.
- [71] A. Zdziennicka, B. Jańczuk, Thermodynamic parameters of some biosurfactants and surfactants adsorption at water-air interface, *J. Mol. Liq.*, 243 (2017) 236–244.
- [72] L. Lonappan, T. Rouissi, R.K. Das, S.K. Brar, A.A. Ramirez, M. Verma, R.Y. Surampalli, J.R. Valero, Adsorption of methylene blue on biochar microparticles derived from different waste materials, *Waste Manage.*, 9 (2016) 537–544.
- [73] B.C. Melo, F.A.A. Paulino, V.A. Cardoso, A.G.B. Pereira, A.R. Fajardo, F.H.A. Rodrigues, Cellulose nanowhiskers improve the methylene blue adsorption capacity of chitosan-g-poly(acrylic acid) hydrogel, *Carbohydr. Polym.*, 181 (2018) 358–367.